



# Immobilized exoglycosidase matrix mediated solid phase glycan sequencing

Róbert Farsang<sup>a,1</sup>, Noémi Kovács<sup>b,1</sup>, Márton Szigeti<sup>a</sup>, Hajnalka Jankovics<sup>b</sup>,  
Ferenc Vonderviszt<sup>b</sup>, András Guttman<sup>a,c,\*</sup>

<sup>a</sup> Translational Glycomics Group, Research Institute of Biomolecular and Chemical Engineering, University of Pannonia, Veszprem, Hungary

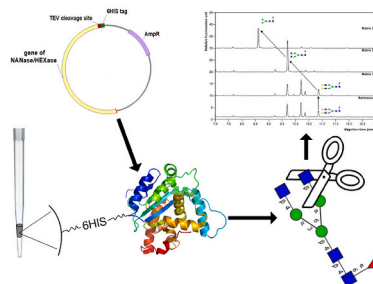
<sup>b</sup> Bio-Nanosystems Laboratory, Research Institute of Biomolecular and Chemical Engineering, University of Pannonia, Veszprem, Hungary

<sup>c</sup> Horváth Csaba Memorial Laboratory of Bioseparation Sciences, Research Center for Molecular Medicine, Faculty of Medicine, Doctoral School of Molecular Medicine, University of Debrecen, Hungary

## HIGHLIGHTS

- Functional exoglycosidase enzymes were designed with attached 6HIS-tag and produced in bacterial expression systems.
- The 6HIS-tagging approach enabled oriented immobilization for enhanced accessibility to the active sites of the enzymes.
- Rapid, high performance enzymatic digestion with immobilized enzymes supporting solid phase glycan sequencing.
- The efficiency of the workflow was demonstrated by N-linked carbohydrate sequencing of biopharma and biological samples.

## GRAPHICAL ABSTRACT



## ARTICLE INFO

### Keywords:

Glycan sequencing  
6HIS-tagged enzyme production  
Exoglycosidases  
Immobilization  
Capillary electrophoresis

## ABSTRACT

Full characterization of the attached carbohydrate moieties of glycoproteins is of high importance for both the rapidly growing biopharmaceutical industry and the biomedical field. In this paper we report the design and production of three important 6HIS-tagged exoglycosidases (neuraminidase,  $\beta$ -galactosidase and hexosaminidase) to support rapid solid phase N-glycan sequencing with high robustness using immobilized enzymes. The exoglycosidases were generated in bacterial expression systems with high yield. Oriented immobilization via the 6HIS-tag portion of the molecules supported easy accessibility to the active sites and consequently high digestion performance. The three exoglycosidases were premixed in an appropriate matrix format and processed in a low-salt buffer to support long term storage. The digestion efficiencies of the immobilized enzymes were

**Abbreviations:** APTS, 8-Aminopyrene-1,3,6-trisulfonic acid trisodium salt; PNGase F, Peptide-N-glycosidase F; CE, capillary electrophoresis; MD, maltodextrin; NANase, neuraminidase-TEV-6HIS enzyme; GALase, 6HIS-TEV- $\beta$ -galactosidase enzyme; HEXase, hexosaminidase-TEV-6HIS enzyme; hIgG1, human immunoglobulin G1.

\* Corresponding author. Translational Glycomics Research Group, Research Institute for Biomolecular and Chemical Engineering, University of Pannonia, 10 Egyetem Street, Veszprem, H-8200, Hungary.

E-mail address: [guttman@mik.uni-pannon.hu](mailto:guttman@mik.uni-pannon.hu) (A. Guttman).

<sup>1</sup> These authors contributed equally.

<https://doi.org/10.1016/j.aca.2022.339906>

Received 5 April 2022; Received in revised form 27 April 2022; Accepted 1 May 2022

Available online 14 May 2022

0003-2670/© 2022 The Authors. Published by Elsevier B.V. This is an open access article under the CC BY-NC-ND license (<http://creativecommons.org/licenses/by-nc-nd/4.0/>).

demonstrated by using solid phase sequencing in conjunction with capillary electrophoresis analysis of the products on a commercial glycoprotein therapeutic (palivizumab) and human serum derived fluorophore labeled glycans.

## 1. Introduction

Protein glycosylation is one of the most common post-translational modifications in eukaryotic cells. It has been known that the attached carbohydrate structures hold a great amount of biological information and, have key roles in cell-cell interactions and signaling pathways, also involved in disease progression [1]. Moreover, N- and O-glycosylation are important for proper folding, stability and the functionality of proteins [2]. The glycan moieties of glycoproteins are composed of monosaccharides, where sugar unit sequence, linkage type and position all contribute to their complexity and diversity. Therefore, structural glycan analysis represents a challenging task, especially in view of their critical importance and understanding of biological function.

The advent of new generation protein therapeutics holds the promise to outperform small molecule drugs due to their outstanding specificity and efficacy. Most often, biotherapeutics are glycosylated such as the frequently used monoclonal antibodies and Fc-fusion proteins. The attached carbohydrates on these therapeutic glycoproteins play key roles in their biological activity, solubility and immunogenicity, so comprehensive characterization of their glycan profiles is of high importance. Currently the most frequently used analytical approaches applied to reveal the structural composition and positional/linkage information of complex carbohydrates include liquid chromatography (LC), capillary electrophoresis (CE) and mass spectrometry (MS), this latter maybe hyphenated with LC or CE [3–5]. Preliminary structural elucidation can be based on the glucose unit (GU) values of the separated components [6–8] that is usually followed by exoglycosidase matrix-based verification [9–15].

Oligosaccharide sequencing by consecutive exoglycosidase digestion steps is one of the most commonly used techniques to determine the structure of complex carbohydrates including recognition of positional and linkage isomers [11,12,16–20]. In other words, since exoglycosidase enzymes have monosaccharide unit and linkage position as well as orientation ( $\alpha$  vs  $\beta$ ) specificity, they can reveal not only the sequence but the associated connection and anomeric configuration information [11, 21]. Exoglycosidase matrix-based glycan sequencing requires separations of the products of each matrix reactions. High performance capillary electrophoresis is frequently used for this task because of its low sample volume requirement, short separation time and multiplexing option [22]. Structural information can be derived from the peak shifts caused by the consecutive exoglycosidase treatments.

One of the limitations of using enzymes in such workflows is that they may rapidly lose their activity, which can significantly increase the cost of analyses. Immobilization of the enzymes reportedly alleviates this handicap [23], furthermore, may enhance enzyme activity and allow repeated use, as well as improves resistance to denaturation [24]. Immobilized trypsin linked to various monolithic supports [25] or capillary walls [26] is frequently used for rapid protein digestion. Temporini et al. developed an on-line pronase immobilized enzyme reactor coupled with HPLC-MS/MS for automated glycoprotein analysis [27]. Immobilization of the pronase enzyme onto an epoxy-silica monolithic material decreased the reaction time from 48 h to 40 min. In an early approach, disposable polymeric nylon tube pipette tips with covalently linked enzymes were used to determine the urea content in serum samples [28]. Subsequently, Nakanishi and co-workers described a trypsin-immobilized pipette tip technique for rapid protein digestion [29]. In the glycomic side, PNGase F-impregnated polyacrylamide gel containing pipette tips were applied to rapid glycoprotein analysis [30]. Krenkova et al. orientedly immobilized PNGase F onto a monolithic support for carbohydrate analysis in capillary electrophoresis [31]. By

all means, selection of the proper immobilization technique to achieve highly efficient enzyme reaction is of high importance because the linking reaction and the orientation influence the catalytic activity of enzymes. Exoglycosidase digestion of glycans typically performed overnight at 37 °C.

In the present study, we report on the design and production of three important 6HIS-tagged exoglycosidases (neuraminidase,  $\beta$ -galactosidase and hexosaminidase) to support rapid solid phase N-glycan sequencing. The use of immobilized exoglycosidases enabled fast and robust oligosaccharide sequencing in conjunction with capillary electrophoresis analysis of the digestion reaction products. The exoglycosidase enzyme digestion steps were optimized by adjusting the enzyme concentration, the digestion buffer pH and the reaction temperature.

## 2. Materials and methods

### 2.1. Chemicals and reagents

Water (HPLC grade), acetonitrile, dithiothreitol (DTT), ammonium acetate, acetic acid, sodium dodecyl sulfate (SDS), sodium cyanoborohydride (1 M in THF), ethylenediaminetetraacetic acid (EDTA), glycine, tetramethylethylenediamine (TEMED), ammonium persulfate (APS) and Nonidet P-40 (NP-40) were obtained from Sigma-Aldrich (St. Louis, MO, USA). Aminopyrene-1,3,6-trisulfonic acid (APTS), the N-linked carbohydrate separation buffer (NCHO) and the M1 magnetic beads of the Fast Glycan Kit were from Bio-Science Kft (Budapest, Hungary). The hlgG1 glycoprotein was from Molecular Innovations (Peary, MI, USA). The palivizumab (Synagis) therapeutic glycoprotein and the human serum were provided by University of Debrecen (Debrecen, Hungary). PNGase F enzyme was produced in house as described in Ref. [32]. Tris-HCl and NaCl were from VWR (Radnor, Pennsylvania, USA).  $\text{NaH}_2\text{PO}_4$  was from Spektrum 3D (Debrecen, Hungary). Glycerol, Coomassie Brilliant Blue R250 and imidazole were from Merck (Darmstadt, Germany). The 40% (37.5:1) acrylamide: bis-acrylamide solution was from Bio-Rad Laboratories (Hercules, California, USA) and boric acid from Scharlab (Debrecen, Hungary). Expression vectors pET23b and pET17b were purchased from Novagen (Madison, Wisconsin, US). Cloning *E. coli* strain TOP10 was from Invitrogen (Carlsbad, California, USA). Restriction endonucleases AgeI HF, SacI HF, NdeI and XhoI, and the expression host SHuffle T7 Express Competent *E. coli* was purchased from New England Biolabs (Ipswich, Massachusetts, USA). BL21-CodonPlus (DE3)-RIL *E. coli* cells originated from Agilent Technologies (Santa Clara, California, USA). T4 DNA ligase was from Thermo Scientific (Waltham, Massachusetts, USA). Cells were cultured in LB Broth medium and LB Agar (Scharlau, Barcelona, Spain). Ampicillin (Amp) and Chloramphenicol (Chl) were from Sigma-Aldrich. A 100 g/L Amp and a 30 g/L Chl stock solution was prepared and used in a 1,000-times dilution in the culture media. Coding DNA sequence of the functional part of neuraminidase and hexosaminidase were synthesized by Biomatik (Cambridge, Ontario, Canada) and provided in pUC57 plasmid. Coding sequence of the functional part of  $\beta$ -galactosidase was synthesized by Twist Bioscience (San Francisco, California, USA) and provided in pTwist plasmid. DNA sequencing was performed by Macrogen Europe (Amsterdam, the Netherlands).

### 2.2. Exoglycosidase enzyme production

#### 2.2.1. Construction of the exoglycosidase expressing plasmids

The coding sequence of the 39–990 polypeptide segment of neuraminidase (the native protein without its releasing signal peptide) from

*sia-AU* gene from *Paenarthrobacter urefaciens* (UniProt ID: Q5W7Q2) and the coding sequence of 34–1,280 polypeptide segment of  $\beta$ -N-acetylhexosaminidase (sequence of the native protein without its releasing signal peptide, the LPXTG recognition signal of sortase and the C-terminal peptidoglycan anchor) from *strH* gene from *Streptococcus pneumoniae serotype 4* (UniProt ID: P49610) were codon optimized for *E. coli* and expanded with the *SacI* nuclease as well as the TEV protease cleavage site coding sequences at their 3'-ends. The synthesized genes were obtained in pUC57 between its *EcoRV* sites. These plasmids and the pET23b expression vector were digested by *NdeI* and *XhoI* restriction enzymes, purified from agarose gel and ligated by T4 ligase, fusing a C-terminal 6HIS-tag coding sequence to the designed gene. TOP10 *E. coli* cells were transformed by the ligation mixture and spread on LB Agar plates containing 100  $\mu$ g/mL Ampicillin. Plasmid DNA from selected colonies was purified by Monarch Plasmid Miniprep Kit (New England Biolabs) and analyzed by restriction digestion and sequencing. The coding sequence of the 137–985 polypeptide segment of  $\beta$ -galactosidase (the catalytic domain of the native enzyme) from *bgaA* gene from *Streptococcus pneumoniae serotype 4* (UniProt ID: Q8DQP4) was first codon optimized for *E. coli*. The synthesized gene was provided in pTwist plasmid and digested by *AgeI* HF and *SacI* HF restriction enzymes. The pET17b plasmid was modified in our laboratory by inserting the coding sequences of an N-terminal 6-HISidine tag, a TEV protease cleavage site, a folding enhancer glycine-serine-histidine (GSH) tripeptide and an *AgeI* restriction nuclease cleavage site by stepwise mutagenesis after the start codon, resulting in the N-terminal polypeptide MHHHHHHEN-LYFQGSHTG fused to the catalytic domain of  $\beta$ -galactosidase, similar to as in Ref. [32].

### 2.2.2. Expression of the exoglycosidases

Neuraminidase-TEV-6HIS (NANase) and hexosaminidase-TEV-6HIS (HEXase) coding pET23b plasmids were used to transform the SHuffle T7 Competent *E. coli* cells, applying the standard protocol recommended by the manufacturer. Protein expression was performed as follows: a 5.0 mL LB/Amp medium was inoculated and grown overnight at 30 °C (250 rpm). 0.5–0.75 L LB/Amp was supplemented with 1.0% (v/v) overnight culture and grown at 30 °C until OD<sub>600</sub> reached 0.6–0.8. Cell culture was induced by 0.4 mM IPTG and further incubated at 16 °C, for 16 h. Cells were harvested by centrifugation at 10,000 g (30 min at 6.0 °C) using a Heraeus Biofuge primo R centrifuge (Hanau, Germany) and subsequently kept at –80 °C. The 6HIS-TEV-GSH-galactosidase (GALase) coding pET17b plasmid was used to transform the BL21-CodonPlus (DE3)-RIL *E. coli* competent bacteria. Cells were grown in 5.0 mL LB/Amp, Chl media overnight at 37 °C (250 rpm). 0.25 L LB/Amp, Chl was inoculated with 0.5% (v/v) overnight culture and grown at 37 °C (250 rpm). When the OD<sub>600</sub> value of the culture reached 0.6–0.8, it was induced with 0.5 mM IPTG and further incubated for 16 h at 30 °C. The cells were harvested by centrifugation by 4,370 g (Heraeus Multifuge 3S-R) for 30 min at 6.0 °C, and kept at –80 °C.

### 2.2.3. Purification of the recombinant exoglycosidases

The cell pellets from the 0.5 L SHuffle/NANase and the 0.75 L SHuffle/HEXase producing cell cultures were thawed and suspended in 10 mL and 15 mL ice-cold buffer 'A' (20 mM NaH<sub>2</sub>PO<sub>4</sub>, 500 mM NaCl, 25 mM imidazole, pH 7.5), respectively, supplemented with Complete protease inhibitor (Hoffman-La Roche, Basel, Switzerland) and incubated on ice for an hour. After addition of 2.0% (w/v) glass beads (diameter 0.5 mm, Sigma-Aldrich) the cells were disrupted by sonication (Cole-Parmer, Vernon Hills, Illinois, USA) 10 times for 30 s by applying 10 W power. The remaining cell debris were settled by ultracentrifugation at 111,000 g for 30 min at 10 °C in a Beckman Coulter Optima™ Max-XP Ultracentrifuge (Brea, CA, USA) using an MLA-80 fixed-angle rotor. The supernatant was filtered through a 0.45  $\mu$ m diameter syringe filter and applied directly to a pre-equilibrated 5 mL HiTrap Chelating Ni-affinity column (GE Healthcare, Chicago, IL, USA). NANase was eluted with 50% 'B' (buffer 'B': 20 mM NaH<sub>2</sub>PO<sub>4</sub>, 500 mM NaCl, 500

mM imidazole, pH 7.5) buffer, which corresponds to ca. 260 mM imidazole, while HEXase was eluted as a single peak at 25% 'B' (ca. 140 mM imidazole).

Cell pellet from 0.25 L cell culture producing BL21-CodonPlus (DE3)-RIL/GALase was thawed and suspended in 10 mL buffer 'A' supplemented with Complete protease inhibitor and incubated on ice for an hour. 2% (w/v) glass beads were added, and the cells were disrupted by sonication 10 times for 30 s by applying 10 W power. The remaining cell debris was settled by ultracentrifugation at 111,000 g for 30 min at 10 °C on an Optima™ Max-XP Ultracentrifuge (Beckman Coulter). The supernatant was filtered through a 0.45  $\mu$ m diameter syringe filter and applied directly to a pre-equilibrated 5.0 mL HiTrap Chelating Ni-affinity column (GE Healthcare). The main proportion of the pure protein was eluted by 125 mM buffered imidazole corresponding to 20% 'B' buffer.

Purity of the proteins in the eluted fractions were checked by SDS PAGE (varied between 8% and 10% based on protein size). The protein concentration was calculated from the absorbance measured at 280 nm on a UV-Vis spectrophotometer (Jasco V-630, Tokyo, Japan) using the following parameters: molecular weight MW = 102.14 kDa, molar extinction coefficient  $\epsilon$  = 114,515 M<sup>-1</sup>cm<sup>-1</sup> for NANase, MW = 139.65 kDa and  $\epsilon$  = 154,940 M<sup>-1</sup>cm<sup>-1</sup> for HEXase and MW = 98.37 kDa,  $\epsilon$  = 175,560 M<sup>-1</sup>cm<sup>-1</sup> for GALase.

### 2.3. N-glycan sample preparation

N-glycan sample preparation utilized 10  $\mu$ L of 10 mg/mL glycoprotein solution (hIgG1, palivizumab) or 10  $\mu$ L human serum at 50-fold aqueous dilution based on Reider et al. [33]. Briefly, the glycoprotein samples were denatured at 80 °C for 10 min using 2.0  $\mu$ L of a denaturation mixture (12.5 mM DTT, 0.6% SDS and 0.06% NP-40). After the denaturation step, the sample was digested with 1.0  $\mu$ L of PNGase F (0.1 mg/mL) in 20  $\mu$ L of 20 mM ammonium acetate at 37 °C for 2.0 h. After the digestion step, 20  $\mu$ L of labeling solution was added containing 6.0 mM of APTS, 100 mM of sodium cyanoborohydride in 1 M THF and 24% (v/v) of acetic acid followed by overnight incubation at 37 °C with the vial lid open. Next, the excess dye was removed using 20  $\mu$ L of tenfold concentrated M1 beads (Fast Glycan Kit) and 185  $\mu$ L of acetonitrile alternately in a total of 4 wash cycles. Then, the APTS labeled sample was eluted using 100  $\mu$ L of HPLC grade water.

### 2.4. Enzyme matrix and co-dialysis

Enzyme solutions were first prepared in matrices [19,34] containing enzymes at concentrations twenty times higher than those required for the deglycosylation reactions, based on preliminary experiments targeting optimal enzyme concentration to complete the enzymatic reaction in 1.0 h at 37 °C. Three different solution compositions were prepared: Matrix 1: NANase only (0.3 mg/mL); Matrix 2: NANase (0.3 mg/mL) + GALase (0.3 mg/mL), and Matrix 3: NANase (0.3 mg/mL) + GALase (0.3 mg/mL) + HEXase (0.42 mg/mL). The exoglycosidase solutions were dialyzed together against 20 mM Tris-HCl, 50 mM NaCl (pH 7.5) buffer at 4.0 °C overnight. Finally, glycerol was added to the dialyzed solutions at the final concentration of 50% (v/v) in order to facilitate long term (up to 2 years) storage at –20 °C.

### 2.5. Enzyme immobilization and exoglycosidase digestion

For all N-glycan sequencing reactions by immobilized 6HIS-tagged exoglycosidase enzymes, one mL size Ni-IMAC resin filled (40  $\mu$ L bed volume) tips were used (PhyNexus, San Jose, CA, USA). Pipetting was done automatically employing 1000+ pipette heads with the controller software (Capture – Purify – Enrich, Version 2.2.3, PhyNexus). The tips (one for each of the three enzyme matrices – see section 2.4.) were washed prior to use with 1.0 mL of 20 mM ammonium acetate solution (pH 7.0) using 1.4 mL/min aspiration and 2.8 mL/min dispensing speeds

(700  $\mu\text{L}$  total volume) for 2.0 min. Then, 10  $\mu\text{L}$  of each enzyme matrix solution was added to 90  $\mu\text{L}$  of HPLC grade water (10x dilution) and immobilized onto the pre-washed tips using 0.6 mL/min aspiration and 1.2 mL/min dispense speeds for 20 min using 300  $\mu\text{L}$  pipetting volume to ensure extensive contact between the enzyme and the resin. Finally, the pipette tips were washed again with 1.0 mL of fresh 20 mM ammonium acetate solution (pH 7.0) using the same conditions as described for the tip wash above. For longer storage, the prepared tips were kept in 50% glycerol containing dialysis buffer (see section 2.4.) up to one month (tested time period) between 2 and 8  $^{\circ}\text{C}$ . The released and APTS labeled N-glycan samples were aliquoted to 20  $\mu\text{L}$  portions and diluted to 100  $\mu\text{L}$  with 10 mM ammonium acetate buffer resulting in the pH of 5.5. Then, the enzyme containing tips (Matrix 1, 2 and 3) were applied for exoglycosidase digestion by using the same pipetting conditions as in the enzyme immobilization step for 30 min at the optimized temperature gradient approach of: 1 – keeping at 37  $^{\circ}\text{C}$  for 5.0 min, 2 - heating up to 50  $^{\circ}\text{C}$  in 3.0 min, 3 - keeping at 50  $^{\circ}\text{C}$  for 12 min, 4 - heating up to 60  $^{\circ}\text{C}$  in 3.0 min, and 5 - keeping at 60  $^{\circ}\text{C}$  for 7.0 min. The schematic representation of the workflow is shown in Fig. 1. The aqueous phase reference digestion experiments were carried out using the same parameters by adding 5  $\mu\text{L}$  of each enzyme matrices to 10  $\mu\text{L}$  sample.

## 2.6. Glycan sequencing by capillary gel electrophoresis

All capillary gel electrophoresis separations were performed on a P/ACE MDQ capillary electrophoresis system, equipped with a laser-induced fluorescence (LIF) detection system (488 nm excitation and 520 nm emission, Beckman Coulter). For all separations, the NCHO matrix was used as separation medium in 50  $\mu\text{m}$  ID bare fused silica capillary columns with 50 cm total length (40 cm effective length). Sample injection: 5.0 psi for 5.0 s. The temperature of capillary and the sample storage compartment were both set at 20  $^{\circ}\text{C}$ . The applied electric field strength during the separations was 600 V/cm with reverse polarity (anode at the inlet capillary end) separation mode.

## 3. Results and discussion

### 3.1. Gene design and construction

Genes for neuraminidase (EC 3.2.1.18), hexosaminidase (EC 3.2.1.52) and  $\beta$ -galactosidase (EC 3.2.1.23) were designed to possess a 6HIS-tag to enable oriented immobilization, utilizing available structural models from the literature to determine their optimal position. In all

instances tagging positions were chosen to be the farthest from the active centers of enzymes (NANase [35], GALase [36], HEXase [37, 38]).

Considering the localization of the active center, the 6HIS-tag followed by a TEV protease cleavage site was fused to the C-terminal end of the enzymatically functional part of neuraminidase and hexosaminidase. For the expression of these two enzymes, the corresponding genes were incorporated into an engineered pET23b plasmid between the *NdeI* and *XhoI* sites, resulting in the pET23b-*NdeI*-neuraminidase-TEV-6HIS-*XhoI* and *NdeI*-hexosaminidase-TEV-6HIS-*XhoI* constructs as shown in Fig. 2 (left panel). In the case of  $\beta$ -galactosidase, similar structural considerations led to the fusion of an N-terminal 6HIS-TEV-tag to its functional part using an engineered pET17b-based plasmid [32] for the expression of GALase (Fig. 2, right panel).

### 3.2. Protein expression in *E. coli* BL21 strains

The six cysteins of NANase form three disulfide bridges at proper folding by oxidation, which is not supported in the reducing environment of the bacterial cytosol. Engineered *E. coli* cells, such as SHuffle T7 Express support appropriate disulfide bridge formation resulting in soluble and catalytically active enzymes. Therefore, our attempt to express NANase in the right form was highly successful yielding about 50 mg pure and soluble protein per liter culture. Since HEXase contains only a single Cys, SHuffle T7 Express also supported right folding by preventing the formation of intermolecular disulfide bonds, resulting in a soluble and catalytically active enzyme. With our approach, 35 mg/L culture pure and properly folded HEXase was obtained. Since SHuffle usually produces significantly lower amount of cell mass, induced cultures were harvested by using higher centrifugal force (10,000 g). GALase does not contain any cysteines, so expression of this enzyme was attempted in four different BL21 (DE3) strains and the CodonPlus (DE3)-RIL was found to be the most effective (74 mg pure and soluble protein per liter culture).

### 3.3. Exoglycosidase concentration optimization and co-dialysis

The optimal digestion reaction concentrations of each enzyme, i.e., to assure complete digestion of the fluorophore labeled glycans, were determined by preliminary aqueous phase experiments with consecutive enzyme by enzyme application. It is important to note that in exoglycosidase enzyme digestion based N-glycan sequencing, only complete digestion is acceptable to ensure unambiguous peak identification. The

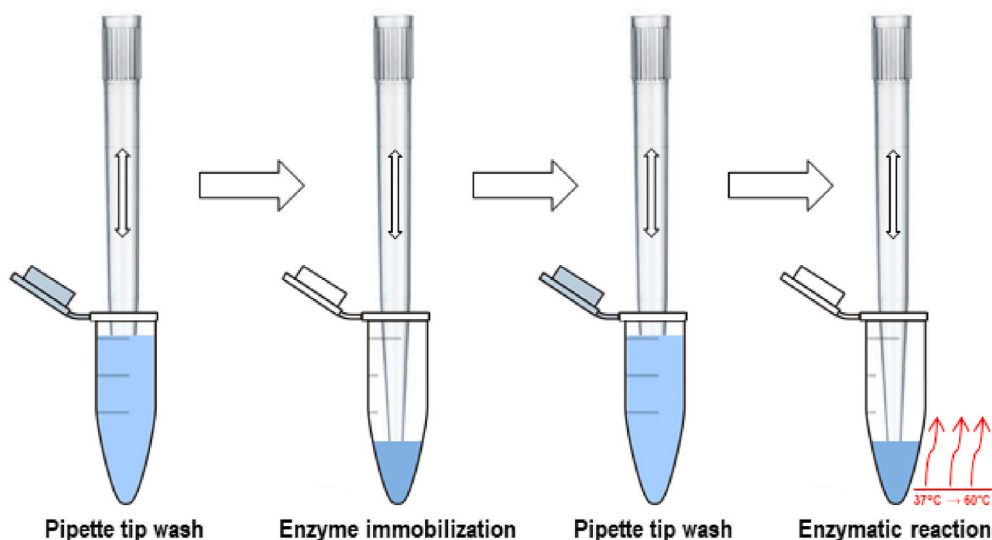


Fig. 1. Schematic representation of the immobilized exoglycosidase digestion workflow.

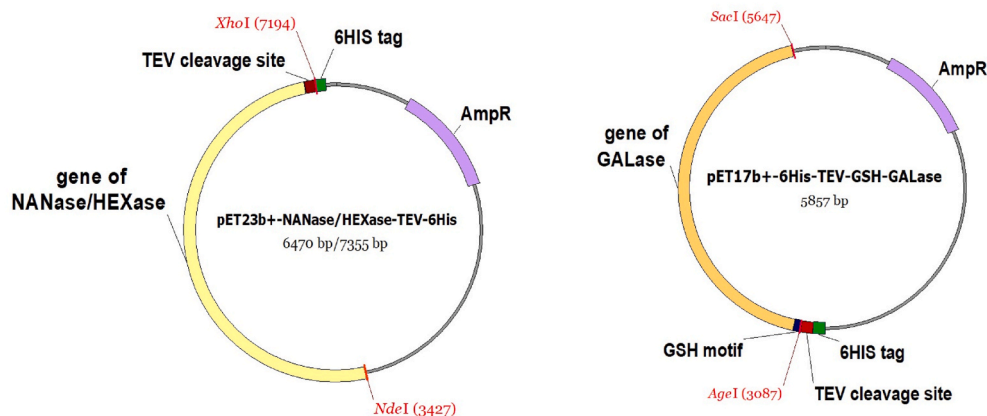


Fig. 2. Gene design for NANase and HEXase (left), as well as GALase (right).

initial target reaction time was set to 1.0 h and the optimal enzyme concentration was 0.15  $\mu\text{M}$  for each enzyme. To generate a stock solution for matrix reactions, the exoglycosidases were pre-mixed with 3.0  $\mu\text{M}$  final concentration each and co-dialyzed against 20 mM Tris-HCl (pH 7.5) buffer containing 50 mM NaCl in order to have the same amount of salt in each member of the matrix, i.e., NANase, NANase + GALase and NANase + GALase + HEXase. Then, the matrices were diluted in a 1:1 ratio with glycerol resulting in 10x enzyme concentration and stored at  $-20\text{ }^{\circ}\text{C}$  until use. This approach resulted an option for long term storage of the enzymes (tested time period: 2 years without activity loss; ready to be used after dilution) and negligible salt effect during electrokinetic injection in CE analysis. High performance enzymatic reaction was attained even with the presence of glycerol in the storage solution since the 10-fold dilution of the matrices prior to use reduced its possible inhibition effect to a negligible level. The efficiency of the 10x diluted co-dialyzed enzyme matrices has been compared to the mixture of the individually used and glycerol-free enzymes using the very same enzyme concentrations at  $37\text{ }^{\circ}\text{C}$  overnight incubation. Multiple batches of enzyme fermentations were tested and compared throughout the development period resulting negligible differences both in yield and performance. Conceptual analysis was outside of the scope of this project.

Fig. 3 compares the CE-LIF traces from the consecutive analyses, normalized by size to the maltose internal standard peak of the non-digested reference sample run in case of the individually applied non-dialyzed enzymes. The % peak areas of the major hlgG1 glycans ( $>1\%$ ) were evaluated and compared between the two set of experiments to determine whether the storage and/or co-dialysis influenced the efficiency of the digestion reactions. The major N-glycan structures

affected by the exoglycosidase treatments in each sequencing stage are listed in Table 1.

The results in Fig. 3 and Table 1 show no significant differences in % peak areas between the individual (standard) and the co-dialyzed enzyme (stored in 1:1 glycerol) approach. Thus, the established storage and pre-mixing method was used in all downstream experiments.

#### 3.4. Comparison of aqueous and solid phase exoglycosidase digestion

Similar to our former approach, all aqueous enzyme reactions using the three 6His-tagged enzyme matrices utilized the temperature gradient digestion protocol as described in Ref. [19]. Furthermore, in order to optimize the combined efficiency of the enzymes, the pH of the samples was adjusted with 10 mM ammonium acetate solution. This was important in order to facilitate the hexosaminidase digestion (pH optimum 5.5), which had the lowest reaction speed among the three enzymes applied. Albeit, this pH was somewhat sub-optimal for the neuraminidase and galactosidase, it was still within their adequate working range. Since the accessibility of the enzymes may be differentially affected by immobilization, the formerly published digestion temperature gradient protocol [19] had to be further optimized as: 1)  $37\text{ }^{\circ}\text{C}$  for 5.0 min, 2) heating up to  $50\text{ }^{\circ}\text{C}$  in 3.0 min, 3) keeping at  $50\text{ }^{\circ}\text{C}$  for 12 min, 4) heating up to  $60\text{ }^{\circ}\text{C}$  in 3.0 min, and 5) keeping at  $60\text{ }^{\circ}\text{C}$  for 7.0 min, to ensure complete and rapid (only 30 min) processing of N-glycan sequencing. The basis of the optimization process was to determine the temperature ranges that would provide the optimal reaction rates for each enzyme and offers a consecutive digestion sequence. For example, while NANase requires only 5.0 min at  $37\text{ }^{\circ}\text{C}$  for complete digestion but does not operate above  $50\text{ }^{\circ}\text{C}$ , the reaction speed

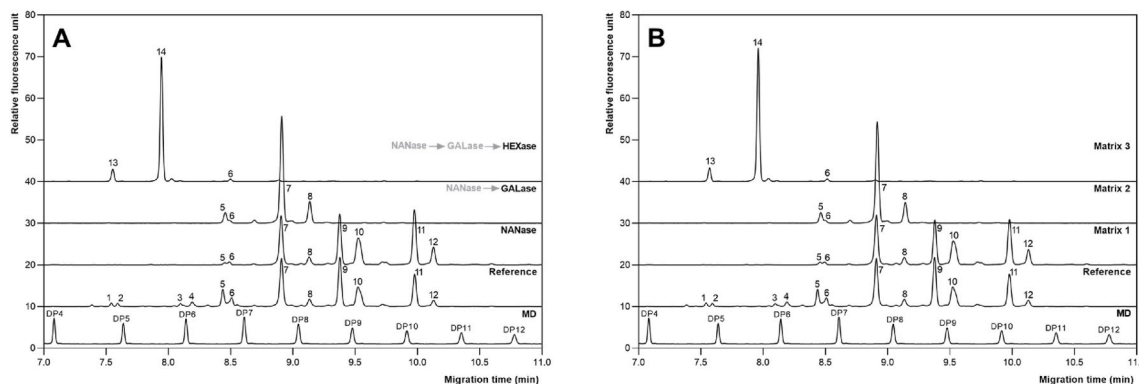


Fig. 3. Oligosaccharide sequencing of PNGase F released and APTS labeled hlgG1 N-glycans with overnight digestion at  $37\text{ }^{\circ}\text{C}$ . The enzymes were applied individually in each consecutive reaction (Panel A) or pre-mixed/co-dialyzed (Panel B). Separation conditions: 50 cm total (40 cm effective) length BFS capillary, NCHO separation matrix,  $20\text{ }^{\circ}\text{C}$  capillary and sample compartment temperature, pressure injection: 5.0 psi for 5.0 s.

**Table 1**

The resulted % peak areas during N-glycan sequencing of the hIgG1 sample. The results of the individually used enzymes (standard) are compared to the co-dialyzed enzyme reactions.

Peak no.	Structure	Migration time (min)	GU value	% peak area	Peak no.	Structure	% peak area	
							Standard	Co-dialyzed
<b>Reference</b>					<b>Neuraminidase digestion</b>			
1	FA2G2S2	7.54	4.85	1.04	7	FA2	22.43	22.47
2	FA2BG2S2	7.59	4.94	0.93	8	FA2B	3.41	3.63
3	FA2G1S1	8.10	5.94	0.95	9	FA2 [6]G1	21.94	21.68
4	A2G1S1	8.19	6.13	1.79	10	FA2 [3]G1	18.47	18.58
5	FA2G2S1/A2	8.44	6.66	7.02	11	FA2G2	25.65	25.97
6	FA2BG2S1/M5	8.50	6.81	4.94	12	FA2BG2	8.09	7.67
7	FA2	8.91	7.72	23.55	<b>Galactosidase digestion</b>			
8	FA2B	9.13	8.24	3.33	7	FA2	83.45	83.24
9	FA2 [6]G1	9.38	8.80	23.01	8	FA2B	16.55	16.76
10	FA2 [3]G1	9.53	9.14	14.52	<b>Hexosaminidase digestion</b>			
11	FA2G2	9.98	10.18	15.98	13	M3	9.60	9.48
12	FA2BG2	10.13	10.53	2.94	14	FM3	90.40	90.52

of GALase and HEXase were significantly higher at higher temperatures.

The immobilized enzymes in the pipette tip microcolumns were then evaluated by using the same digestion parameters as above. Although, the individually immobilized GALase and NANase enzymes resulted in complete digestion in 30 min using the temperature gradient method (Fig. 4, traces Matrix 1 and 2), the HEXase enzyme showed incomplete digestion in its immobilized form when it was in the matrix in the same concentration as the other two (Fig. 4, Matrix 3#1 trace). As a first approximation, we considered that the three enzymes competed for the available Ni(II) binding sites and the HEXase was the less effective. Therefore, we increased the HEXase concentration to 0.6  $\mu$ M (four-fold). With this modification, complete hexosaminidase digestion was obtained in 30 min using the immobilized enzymes as shown in Fig. 4, Matrix 3#2 trace. It is important to note that this solid state sequencing approach opens up the opportunity for full automation using liquid handling robots with immobilized enzyme containing pipette tip microcolumns.

In addition, we found that the HEXase had the lowest activity among the applied enzymes (data not shown) in the matrices. This exoglycosidase was  $\sim$ 40 kDa larger than the NANase and GALase due the G5 spacer module of the source enzyme [38], which was designed to

optimize the orientation of the double active centrum during immobilized operation. This increased size probably represented an additional disadvantage during the co-immobilization process and necessitated the use of extra amount of HEXase in Matrix 3. It is important to note that the amount of the immobilized enzyme was significantly below the LOQ of our detection systems [32]. More importantly, exoglycosidase based glycan sequencing requires complete digestion within the given time frame, otherwise the obtained results can be ambiguous.

### 3.5. Solid phase glycan sequencing of a therapeutic monoclonal antibody and human serum N-glycans

To evaluate our novel solid phase oligosaccharide sequencing approach, a human serum (Fig. 5A) and a monoclonal antibody therapeutic (palivizumab, Fig. 5B) were tested with the premixed and co-dialyzed exoglycosidase enzymes in immobilized format using the optimized 30 min temperature gradient method as described above. In all instances, complete digestion was obtained in the given timeframe as shown in the panels of Fig. 5. The arrows highlight examples of the digestion mediated consecutive structural changes of a representative N-glycan in each panel. Important to note that the same digestion

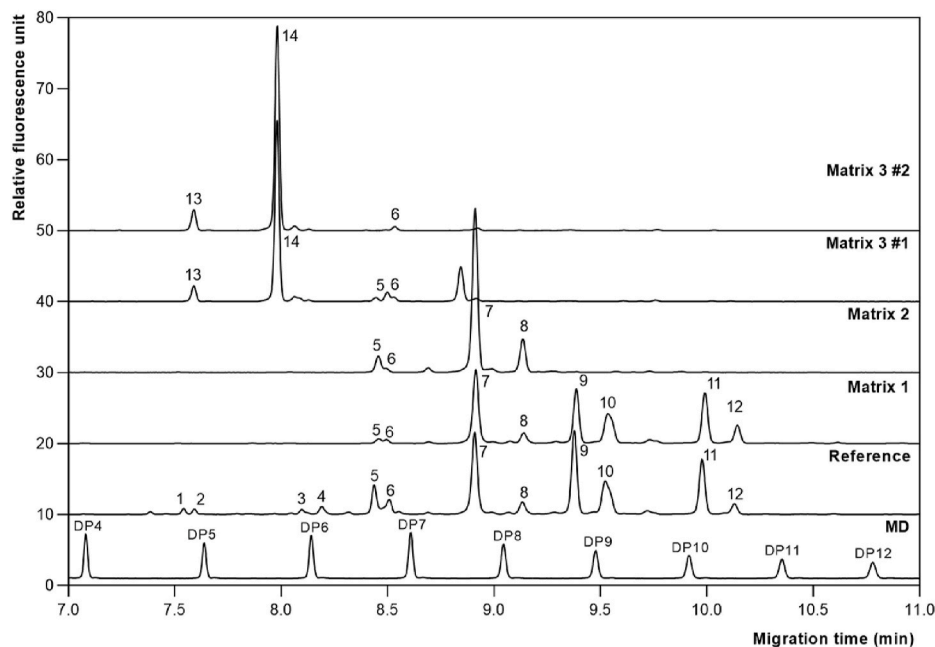


**Fig. 4.** Exoglycosidase digestion based solid phase sequencing of the PNGase F released and APTS labeled hIgG1 N-glycans using immobilized enzyme matrices. Separation conditions and peak assignments are the same as in Fig. 2.

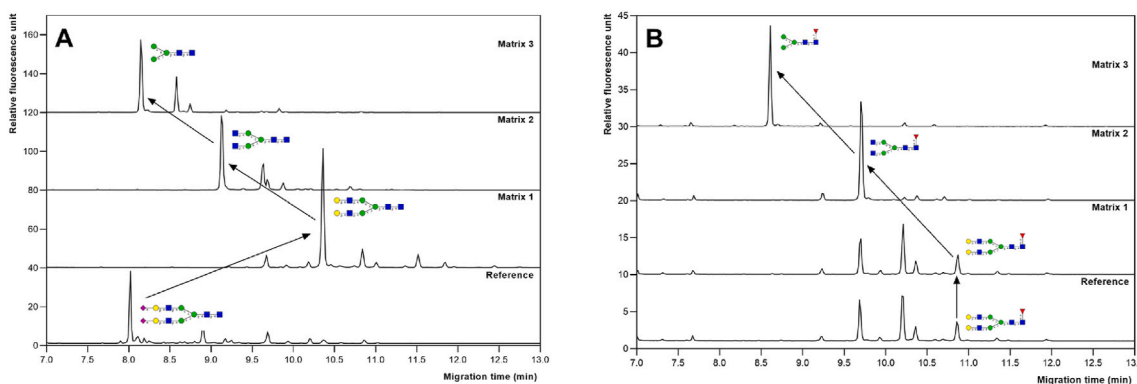


**Fig. 5.** Solid phase N-glycan sequencing of PNGase F released and APTS labeled N-glycans from human serum (panel A) and palivizumab (panel B). The arrows highlight examples of the digestion mediated consecutive structural changes of a representative N-glycan in each panel. Separation conditions were the same as in Fig. 2.

efficiency was obtained in aqueous phase (non immobilized) reactions using the same 6HIS-tagged enzymes under the conditions described above (data not shown), thus, the immobilization did not decrease the efficiency of the enzymes.

#### 4. Conclusions

In this work, we first designed and produced three important 6HIS-tagged exoglycosidase enzymes including neuraminidase,  $\beta$ -galactosidase and hexosaminidase in order to rapidly perform solid phase N-glycan sequencing with high robustness. Functional exoglycosidase enzymes were produced in high yield and purity using bacterial expression systems in a cost-effective manner. The co-expressed 6HIS-tag enabled oriented immobilization to ensure enhanced accessibility to the active sites of the enzymes, therefore, high performance digestion both in aqueous phase and in immobilized formats. This latter can readily accommodate automation with liquid handling robots for high throughput workflows. The enzymes were premixed in matrices, similar to former applications [34] and more importantly, co-dialyzed against a common low salt concentration buffer in order to support long term storage of the ready to use pre-mixed solutions. This step also reduced the negative effect of the high conductivity buffer ingredients on signal strength during electrokinetic injection in capillary electrophoresis analysis. The workflow with our novel solid phase oligosaccharide sequencing approach was successfully demonstrated on a commercially available therapeutic monoclonal antibody and human serum sample.

#### Funding

Direct funding is not applicable.

#### Ethical approval

Ethical approval is not applicable.

#### Informed consent

Informed consent is not applicable.

#### CRedit authorship contribution statement

**Róbert Farsang:** experimental work. **Noémi Kovács:** protein design, experimental work. **Márton Szigeti:** Writing – original draft, Separation system development, writing. **Hajnalka Jankovics:** Writing – original draft, Exoglycosidase gene design, writing. **Ferenc Vonderviszt:** Supervision, Writing – review & editing, and review and. **András Guttman:** Supervision, Writing – review & editing, writing review and

editing.

#### Declaration of competing interest

The authors declare that they have no known competing financial interests or personal relationships that could have appeared to influence the work reported in this paper.

#### Acknowledgment

The authors gratefully acknowledge the support of the BIO-NANO\_GINOP-2.3.2-15-2016-00017 project, by the TKP2020-IKA-07 project financed under the 2020-4.1.1-TKP2020 Thematic Excellence Programme by the National Research, Development and Innovation Fund of Hungary and the V4-Korea Joint Research Program, project National Research Development and Innovation Office (NKFIH) (NN 127062) grants of the Hungarian Government. This is contribution #192 from the Horváth Csaba Memorial Laboratory of Bioseparation Sciences.

#### References

- [1] H.J. Gabius, The sugar code: why glycans are so important, *Biosystems* 164 (2018) 102–111, <https://doi.org/10.1016/j.biosystems.2017.07.003>.
- [2] J.F. Vliegthart, The complexity of glycoprotein-derived glycans, *Proc. Jpn. Acad. Ser. B Phys. Biol. Sci.* 93 (2017) 64–86, <https://doi.org/10.2183/pjab.93.005>.
- [3] W. Qin, H. Pei, R. Qin, R. Zhao, J. Han, Z. Zhang, K. Dong, S. Ren, J. Gu, Alteration of serum IgG galactosylation as a potential biomarker for diagnosis of neuroblastoma, *J. Cancer* 9 (2018) 906–913, <https://doi.org/10.7150/jca.22014>.
- [4] D.J. Ashline, A.J. Lapadula, Y.H. Liu, M. Lin, M. Grace, B. Pramanik, V.N. Reinhold, Carbohydrate structural isomers analyzed by sequential mass spectrometry, *Anal. Chem.* 79 (2007) 3830–3842, <https://doi.org/10.1021/ac062383a>.
- [5] D.M. Sheeley, V.N. Reinhold, Structural characterization of carbohydrate sequence, linkage, and branching in a quadrupole ion trap mass spectrometer: neutral oligosaccharides and N-linked glycans, *Anal. Chem.* 70 (1998) 3053–3059, <https://doi.org/10.1021/ac9713058>.
- [6] S. Mittermayr, A. Guttman, Influence of molecular configuration and conformation on the electromigration of oligosaccharides in narrow bore capillaries, *Electrophoresis* 33 (2012) 1000–1007, <https://doi.org/10.1002/elps.201100681>.
- [7] G. Jarvas, M. Szigeti, A. Guttman, Structural identification of N-linked carbohydrates using the GÜcal application: a tutorial, *J. Proteomics* 171 (2018) 107–115, <https://doi.org/10.1016/j.jprot.2017.08.017>.
- [8] G. Jarvas, M. Szigeti, J. Chapman, A. Guttman, Triple-internal standard based glycan structural assignment method for capillary electrophoresis analysis of carbohydrates, *Anal. Chem.* 88 (2016) 11364–11367, <https://doi.org/10.1021/acs.analchem.6b03596>.
- [9] C.T. Thiesler, S. Cajic, D. Hoffmann, C. Thiel, L. van Diepen, R. Hennig, M. Sgodda, R. Weimann, U. Reichl, D. Steinemann, U. Diekmann, N.M. Huber, A. Oberbeck, T. Cantz, A.W. Kuss, C. Körner, A. Schambach, E. Rapp, F.F. Buettner, Glycomic characterization of induced pluripotent stem cells derived from a patient suffering from phosphomannomutase 2 congenital disorder of glycosylation (PMM2-CDG), *Mol. Cell. Proteomics* : MCP 15 (2016) 1435–1452, <https://doi.org/10.1074/mcp.M115.054122>.
- [10] R. Hennig, S. Cajic, M. Borowiak, M. Hoffmann, R. Kottler, U. Reichl, E. Rapp, Towards personalized diagnostics via longitudinal study of the human plasma N-glycome, *Biochim. Biophys. Acta* 1860 (2016) 1728–1738, <https://doi.org/10.1016/j.bbagen.2016.03.035>.

- [11] S. Gattu, C.L. Crihfield, L.A. Holland, Microscale measurements of michaelis-menten constants of neuraminidase with nanogel capillary electrophoresis for the determination of the sialic acid linkage, *Anal. Chem.* 89 (2017) 929–936, <https://doi.org/10.1021/acs.analchem.6b04074>.
- [12] S.A. Archer-Hartmann, L.M. Sargent, D.T. Lowry, L.A. Holland, Microscale exoglycosidase processing and lectin capture of glycans with phospholipid assisted capillary electrophoresis separations, *Anal. Chem.* 83 (2011) 2740–2747, <https://doi.org/10.1021/ac103362r>.
- [13] Y. Mechref, M.V. Novotny, Mass spectrometric mapping and sequencing of N-linked oligosaccharides derived from submicrogram amounts of glycoproteins, *Anal. Chem.* 70 (1998) 455–463, <https://doi.org/10.1021/ac970947s>.
- [14] T. Song, S. Ozcan, A. Becker, C.B. Lebrilla, In-depth method for the characterization of glycosylation in manufactured recombinant monoclonal antibody drugs, *Anal. Chem.* 86 (2014) 5661–5666, <https://doi.org/10.1021/ac501102t>.
- [15] M. Doherty, C.A. McManus, R. Duke, P.M. Rudd, High-throughput quantitative N-glycan analysis of glycoproteins, *Methods Mol. Biol.* 899 (2012) 293–313, [https://doi.org/10.1007/978-1-61779-921-1\\_19](https://doi.org/10.1007/978-1-61779-921-1_19).
- [16] M. Guttman, C. Váradi, K.K. Lee, A. Guttman, Comparative glycoprofiling of HIV gp120 immunogens by capillary electrophoresis and MALDI mass spectrometry, *Electrophoresis* 36 (2015) 1305–1313, <https://doi.org/10.1002/elps.201500054>.
- [17] M. Yamagami, Y. Matsui, T. Hayakawa, S. Yamamoto, M. Kinoshita, S. Suzuki, Plug-plug kinetic capillary electrophoresis for in-capillary exoglycosidase digestion as a profiling tool for the analysis of glycoprotein glycans, *J. Chromatogr., A* 1496 (2017) 157–162, <https://doi.org/10.1016/j.chroma.2017.03.019>.
- [18] C. Váradi, C. Jakes, J. Bones, Analysis of cetuximab N-Glycosylation using multiple fractionation methods and capillary electrophoresis mass spectrometry, *J. Pharmaceut. Biomed. Anal.* 180 (2020), 113035, <https://doi.org/10.1016/j.jpba.2019.113035>.
- [19] M. Szigeti, A. Guttman, Automated N-glycosylation sequencing of biopharmaceuticals by capillary electrophoresis, *Sci. Rep.* 7 (2017) 11663, <https://doi.org/10.1038/s41598-017-11493-6>.
- [20] A. Taga, M. Sugimura, S. Suzuki, S. Honda, Estimation of sialic acid in a sialoglycan and a sialoglycoprotein by capillary electrophoresis with in-capillary sialidase digestion, *J. Chromatogr., A* 954 (2002) 259–266, [https://doi.org/10.1016/s0021-9673\(02\)00151-6](https://doi.org/10.1016/s0021-9673(02)00151-6).
- [21] G. Lu, C.L. Crihfield, S. Gattu, L.M. Veltri, L.A. Holland, Capillary electrophoresis separations of glycans, *Chem. Rev.* 118 (2018) 7867–7885, <https://doi.org/10.1021/acs.chemrev.7b00669>.
- [22] W. Laroy, R. Contreras, N. Callewaert, Glycome mapping on DNA sequencing equipment, *Nat. Protoc.* 1 (2006) 397–405, <https://doi.org/10.1038/nprot.2006.60>.
- [23] R.A. Sheldon, S. van Pelt, Enzyme immobilisation in biocatalysis: why, what and how, *Chem. Soc. Rev.* 42 (2013) 6223–6235, <https://doi.org/10.1039/c3cs60075k>.
- [24] J. Krenková, F. Foret, Immobilized microfluidic enzymatic reactors, *Electrophoresis* 25 (2004) 3550–3563, <https://doi.org/10.1002/elps.200406096>.
- [25] J. Krenkova, N.A. Lacher, F. Svec, Highly efficient enzyme reactors containing trypsin and endoproteinase LysC immobilized on porous polymer monolith coupled to MS suitable for analysis of antibodies, *Anal. Chem.* 81 (2009) 2004–2012, <https://doi.org/10.1021/ac8026564>.
- [26] E.C.A. Stigter, G.J. de Jong, W.P. van Bennekom, Development of an open-tubular trypsin reactor for on-line digestion of proteins, *Anal. Bioanal. Chem.* 389 (2007) 1967–1977, <https://doi.org/10.1007/s00216-007-1584-5>.
- [27] C. Temporini, E. Perani, E. Calleri, L. Dolcini, D. Lubda, G. Caccialanza, G. Massolini, Pronase-immobilized enzyme reactor: an approach for automation in glycoprotein analysis by LC/LC–ESI/MSn, *Anal. Chem.* 79 (2007) 355–363, <https://doi.org/10.1021/ac0611519>.
- [28] P.V. Sundaram, Immobilized-enzyme pipette. Scope and limitations of a simple device, *Biochem. J.* 179 (1979) 445–447, <https://doi.org/10.1042/bj1790445>.
- [29] S. Ota, S. Miyazaki, H. Matsuoka, K. Morisato, Y. Shintani, K. Nakanishi, High-throughput protein digestion by trypsin-immobilized monolithic silica with pipette-tip formula, *J. Biochem. Biophys. Methods* 70 (2007) 57–62, <https://doi.org/10.1016/j.jbbm.2006.10.005>.
- [30] S. Yamamoto, M. Ueda, M. Kasai, Y. Ueda, M. Kinoshita, S. Suzuki, A fast and convenient solid phase preparation method for releasing N-glycans from glycoproteins using trypsin- and peptide-N-glycosidase F (PNGase F)-impregnated polyacrylamide gels fabricated in a pipette tip, *J. Pharmaceut. Biomed. Anal.* 179 (2020), 112995, <https://doi.org/10.1016/j.jpba.2019.112995>.
- [31] J. Krenkova, A. Szekrenyes, Z. Keresztessy, F. Foret, A. Guttman, Oriented immobilization of peptide-N-glycosidase F on a monolithic support for glycosylation analysis, *J. Chromatogr., A* 1322 (2013) 54–61, <https://doi.org/10.1016/j.chroma.2013.10.087>.
- [32] N. Kovács, R. Farsang, M. Szigeti, F. Vonderviszt, H. Jankovics, Enhanced recombinant protein production of soluble, highly active and immobilizable PNGase F, *Mol. Biotechnol.* (2022), <https://doi.org/10.1007/s12033-022-00464-6>.
- [33] B. Reider, M. Szigeti, A. Guttman, Evaporative fluorophore labeling of carbohydrates via reductive amination, *Talanta* 185 (2018) 365–369, <https://doi.org/10.1016/j.talanta.2018.03.101>.
- [34] A. Guttman, Multistage sequencing of N-linked fetuin glycans by capillary gel electrophoresis and enzyme matrix digestion, *Electrophoresis* 18 (1997) 1136–1141, <https://doi.org/10.1002/elps.1150180719>.
- [35] S. Christensen, J. Egebjerg, Cloning, expression and characterization of a sialidase gene from *Arthrobacter ureafaciens*, *Biotechnol. Appl. Biochem.* 41 (2005) 225–231, <https://doi.org/10.1042/ba20040144>.
- [36] A.K. Singh, B. Pluvinae, M.A. Higgins, A.B. Dalia, S.A. Woodiga, M. Flynn, A. R. Lloyd, J.N. Weiser, K.A. Stubbs, A.B. Boraston, S.J. King, Unravelling the multiple functions of the architecturally intricate *Streptococcus pneumoniae*  $\beta$ -galactosidase, BgaA, *PLoS pathogens* 10 (2014), e1004364, <https://doi.org/10.1371/journal.ppat.1004364>.
- [37] B. Pluvinae, M.A. Higgins, D.W. Abbott, C. Robb, A.B. Dalia, L. Deng, J.N. Weiser, T.B. Parsons, A.J. Fairbanks, D.J. Vocadlo, A.B. Boraston, Inhibition of the pneumococcal virulence factor StrH and molecular insights into N-glycan recognition and hydrolysis, *Structure* 19 (2011) 1603–1614, <https://doi.org/10.1016/j.str.2011.08.011> (London, England : 1993).
- [38] B. Pluvinae, S. Chitayat, E. Ficko-Blean, D.W. Abbott, J.M. Kunjachen, J. Grondin, H.L. Spencer, S.P. Smith, A.B. Boraston, Conformational analysis of StrH, the surface-attached exo- $\beta$ -D-N-acetylglucosaminidase from *Streptococcus pneumoniae*, *J. Mol. Biol.* 425 (2013) 334–349, <https://doi.org/10.1016/j.jmb.2012.11.005>.